Zhengyuan prescription inhibits X-ray-induced injury of human umbilical vein endothelial cells by activating the Nrf2 signaling pathway

cheng xiaoni
Shaanxi Finance and Economics College: Xi'an Jiaotong University
Yalei Pan (panyalei588@163.com)
Shaanxi Finance and Economics College: Xi'an Jiaotong University https://orcid.org/0000-0002-3579-4395
Zhishu Tang
Shaanxi University of Chinese Medicine
Rui Zhou
Shaanxi University of Chinese Medicine
Haichao Zhang
Shaanxi University of Chinese Medicine
Jie Su
Shaanxi University of Chinese Medicine
Zhongxing Song
Shaanxi University of Chinese Medicine
Jian Ni
Shaanxi University of Chinese Medicine

Research

Keywords: Zhengyuan Prescription, X-ray, human umbilical vein endothelial cell, oxidative stress

Posted Date: March 6th, 2021

DOI: https://doi.org/10.21203/rs.3.rs-282443/v1

Abstract

Background: Zhengyuan prescription (ZYP) is a Chinese herbal medicine used in clinical practice to protect against radiotherapy-induced injuries. In this study, we investigate the protective effect of ZYP against X-ray-induced injury of human umbilical vein endothelial cells (HUVECs), and we explore the mechanisms underlying this effect.

Methods: After 3 h of ZYP intervention, the cells in the ZYP group were irradiated with 6 Gy X-rays and cultured for 48 h. Subsequently, the cell viability, cell morphology, mitochondrial membrane potential, and apoptosis and oxidative stress markers were observed, as well as the expressions of apoptotic and oxidative stress proteins.

Results: The obtained results demonstrate that exposure to X-rays promotes cell death, reduces mitochondrial membrane potential, and induces the pirroduction of intracellular reactive oxygen species (ROS). Pretreatment with ZYP reverses these effects to a great extent. Moreover, it up-regulates the expression of the B-cell lymphoma 2 (Bcl-2) apoptosis inhibitor protein while down-regulating the expressions of Bcl-2-associated X protein (Bax), caspase-3, and caspase-9. Interestingly, ZYP can also inhibit oxidative stress injury by activating the expression of Nrf2 (Nuclear Factor E2 related factor) regulated antioxidant enzyme genes such as Heme oxygenase 1 (HO-1) and NAD(P)H:quinone oxidoreductase-1 (NQO1)

Conclusions: This study is the first to demonstrate that ZYP suppresses X-ray-induced injury of HUVECs by activating the Nrf2 signaling pathway.

Background

Radiotherapy is an efficient tumor treatment that can effectively prolong the lives of patients and enhance their quality of life [1,2]. In some cases, radiotherapy has resulted in therapeutic outcomes better than those achieved using other available treatments [3]. However, the application of radiotherapy treatment is limited by its side effects, including high toxicity and normal tissue damage [4,5]. The mechanisms underlying the development of these side effects implicate oxidative stress [6]. To minimize the oxidative imbalance effect associated with ionizing radiation and to improve the targeting effect of future radiotherapy treatments, the sensitivity of tumor cells towards ionizing radiation (IR) must be increased, and the effect of this radiation on normal tissues must be reduced [7].

Traditional Chinese medicine (TCM), especially Chinese herbal medicine, has evolved over thousands of years in China, Japan, and other Asian countries. TCM has been used in cancer prevention and treatment therapies, and it has shown good efficiency [8-10]. Moreover, preclinical and clinical studies have shown that the combination of TCM and conventional western medicine (chemotherapy and radiotherapy) can provide effective supportive care for cancer patients [8, 11]. According to TCM theory, the acute injury caused by IR is related to the heat toxicity of the radiation, which consumes qi and yin upon entering the human body [12]. ZYP is a Chinese herbal prescription that is composed of Radix Angelicae Sinensis,

Radix Panacis Quinquefolii, Herba Agrimoniae, Paris polyphylla and Adenophora tetraphylla (Table 1) that may be used to alleviate the symptoms of radiotherapy-induced syndrome by replenishing qi, replenishing blood, clearing heat, and detoxicating [10, 13]. In previous studies, we had shown that ZYP has significant protective effects against 60Co γ-ray induced injury in mice and against cyclophosphamide-induced myelosuppression in guinea pigs [14]. However, the effects and mechanisms of ZYP on X-ray-induced injury remain unclear.

Vascular endothelial cells in blood vessels are highly sensitive to radiation [15]. Normally, these cells regulate the growth of blood vessels, the adhesion and non-adhesion of blood cells, the relaxation and contraction of the vessels, and the balance of anticoagulants and procoagulants [16]. Therefore, they play an important role in maintaining the integrity of the vascular structure, regulating the flow of blood, mediating the inflammatory response, and responding to immunity [17-19]. According to the literature, IR exposure at a certain dose induces morphological changes in vascular endothelial cells, including nuclear enlargement, karyopycnosis, polykaryocyte formation, and decreased cell homogeneity [18, 20]. Moreover, exposure to IR may lead to the activation of human umbilical vein endothelial cells (HUVECs), even in the absence of pathogens (i.e. aseptic inflammation). The exact stimulant causing HUVEC activation probably causes oxidative stress as well [15, 19]. In addition to the aforementioned effects, IR exposure inhibits the antioxidant mechanisms of endothelial cells by promoting ROS production and by threatening the integrity and survival of normal surrounding cells [6]. In this study, we investigate the antioxidant effect of ZYP on X-ray-induced injury of HUVECs, and we analyze the underlying mechanisms.

Materials

Reagents and antibodies

MTT, dimethyl sulfoxide (DMSO), and FITC Phalloidin were acquired from Beijing Solarbio Science & Technology Co., Ltd. (Beijing, China). DAPI was purchased from Sigma Aldrich (St. Louis, MO, United States). The MDA assay, superoxide dismutase (SOD) assay, ROS detection, and LDH assay kits were supplied by Nanjing Jian cheng Biological Engineering Materials Co., Ltd. (Nanjing, Jiangsu, China), whereas the rhodamine 123 staining kit and kFlior555 Click-iT EDU cell proliferation detection kit were purchased from Jiangsu KeyGEN BioTECH Corp., Ltd. (Jiangsu, China). The Calcein/PI cell viability/cytotoxicity assay kit and annexin V-FITC apoptosis assay kit wer bought from Beyotime (Shanghai, China) and Absin (Shanghai, China), respectively.

HPLC analysis

The composition of the five-herb ZYP prescription was verified by HPLC analysis. First, the prescription was boiled for 2 h then filtered. The extraction process was repeated twice, then the extract was concentrated and spray dried. The obtained powder was dissolved in 60% methanol, and the solution was subsequently analyzed by high performance liquid chromatography (HPLC). HPLC-diode array detector (HPLC-DAD) analysis was performed on an Agilent-1260 system coupled with a DAD detector. An Inert

Sustain C18 column (150 mm×4.6 mm, 5 μm) was maintained at a column temperature of 30°C. The mobile phase, consisting of (A) acetonitrile and (B) 0.1% phosphoric acid, was applied in the following linear elution gradient: 0–20 min, 18–18% A; 20–30 min, 18–20% A; 30–35 min, 20–22% A; 35–54 min, 22–32% A; 54–61 min, 32–40% A; 61–62 min, 40–43% A; 62–85 min, 43–44% A; 85–87 min, 44–18% A; and 87–90 min, 18–18% A. The flow rate was 1 mL/min, and the detection wavelength was 203 nm. The injection volume was 10 μL.

Cell culture and treatment

HUVECs purchased from BeNa Culture Collection (Beijing, China) were maintained in Dulbecco's Modified Eagle Medium (DMEM; Biological Industries, Kibbutz Beit Haemek, Israe) supplemented with 15% fetal bovine serum (FBS; Biological Industries, Kibbutz Beit Haemek, Israe). The cells were cultured in an incubator at 37°C, under 5% CO_2 atmosphere, until 80–90% confluency was reached. To evaluate the effects of ZYP on X-ray induced damage, the cells were randomly divided into six groups: A, negative control group; B, X-ray model group; C, X-ray+200 μg/mL vitamin D_2 group; D, X-ray+20 μg/mL ZYP group; E, X-ray+50 μg/mL ZYP group; and F, X-ray+100 μg/mL ZYP group.

Ionizing radiation

The cultured cells were exposed to X-rays issued from an X-ray irradiation system (Elekta, Sweden) equipped with a medical linear accelerator. The samples were divided into six groups irradiated with 0, 4, 6, 8, 10, and 14 Gy ionizing radiation doses at the rate of 300 μ/min.

Annexin V-FITC staining

FITC-labeled phalloidin and DAPI staining were used to detect the cytoskeletal distribution of HUVECs and evaluate the specific morphological changes in the nucleus that induce apoptosis. First, HUVECs were seeded in 6-well plates at the density of 10×10^4 cells/well, after 3 h of ZYP intervention, the cells in the ZYP group were irradiated with 6 Gy X-rays and cultured for 48 h. Afterwards, the cells were fixed with 4% paraformaldehyde for 15 min, followed by treatment with 0.5% Triton X-100 for 5 min. Prior to the addition of the V-FITC working solution, the cells were washed twice with phosphate-buffered saline (PBS), then they were incubated with V-FITC in the dark at 37°C. Thirty minutes later, the cells were again washed twice with PBS, stained with 5 μg/mL DAPI in the dark at 37°C for 15 min, then analyzed using an inverted fluorescence microscope. Representative digital images were acquired for analysis.

Calcein/PI cell assay

FITC-labeled phalloidin and DAPI staining were used to detect the cytoskeletal distribution of HUVECs and evaluate the specific morphological changes in the nucleus that induce apoptosis. First, HUVECs were seeded in 6-well plates at the density of 10×10^4 cells/well, after 3 h of ZYP intervention, the cells in the ZYP group were irradiated with 6 Gy X-rays and cultured for 48 h. Afterwards, the cells were fixed with 4% paraformaldehyde for 15 min, followed by treatment with 0.5% Triton X-100 for 5 min. Prior to the

addition of the V-FITC working solution, the cells were washed twice with phosphate-buffered saline (PBS), then they were incubated with V-FITC in the dark at 37°C. Thirty minutes later, the cells were again washed twice with PBS, stained with 5 μg/mL DAPI in the dark at 37°C for 15 min, then analyzed using an inverted fluorescence microscope. Representative digital images were acquired for analysis.

Cell proliferation detection via EDU labeling

HUVECs were seeded in 6-well plates at the density of 10×10^4 cells/well and treated with positive sources at different concentrations for EDU labeling. Thirty-six hours after X-ray irradiation, the cells were fixed and infiltrated, then they were incubated with the Click-iT reaction mixture for 30 min in the dark. Subsequently, the cells were washed twice with PBS and stained with 5 μg/mL Hoechset for 10 min in the dark. After washing again with PBS (twice), the cells were finally analyzed by inverted fluorescence microscopy. Representative digital images were acquired for analysis.

Determination of mitochondrial membrane potential

HUVECs were cultured, induced X-ray damage and treated with ZYP for 48 h. The cells were incubated with 2 μM rhodamine 123 in the dark at 37°C for 30 min. Next, the cells were washed twice with serum-free medium then incubated in this medium at 37°C, in the dark. Sixty minutes later, the fluorescence of cells was measured using an inverted fluorescence microscope and the cell count and fluorescence intensity were determined using the ImageJ software.

Flow cytometry

To assess the mitochondrial membrane potential, the cells were stained with rhodamine 123, then they were washed with PBS and analyzed by a flow cytometer using BD FACSuite v1.0.6.

Apoptosis was detected using the Annexin-V/PI assay kit (Absin Bioscience Inc). For this purpose, the treated cells were washed with pre-cooled PBS then resuspended in 300 μL 1×Binding Buffer. Subsequently, the cells were stained with 5 μL Annexin V-FITC and 5 μL PI in the dark for 15 min. The apoptotic cells were then detected using flow cytometry, and the proportion (%) of each sub-population of cells was determined using the FlowJo 7.6 software.

Evaluation of LDH, MDA, and SOD levels

The MDA and SOD levels in seeded HUVECs (10×10^4 cells/well in a 6-well plate) were determined according to the thiobarbituric acid and xanthine oxidation methods, respectively. To determine the LDH level, the supernatant of the seeded cells was collected. A microplate reader was used to measure MDA, SOD, and LDH levels based on absorbance values.

Western blotting

Western blot analysis was used to assess changes in the protein expressions of HUVECs after ZYP treatment and X-ray irradiation. After treatment with ZYP, the cells were collected and lysed in RIPA lysis buffer (Beyotime Biotechnology Co., Ltd.), and the protein concentration was quantified using the bicinchoninic acid (BCA) assay. Subsequently, the protein samples were loaded separated by SDS-PAGE and electrophoretically transferred onto PVDF membranes. Incubate the membrane with blocking solution (5% skimmed milk) at room temperature for 1 h. After washing, incubate with the corresponding primary antibody (Table 2) overnight at 4°C. Incubated with a secondary antibody (Cell Signaling Technology) coupled with horseradish peroxidase. Positive antibody binding was then visualized by ECL detection and analyzed by the Image J software (BioRad, Hercules, CA, USA).

Statistical analysis

All of the statistical analyses were carried out using a GraphPad Prism V6 (GraphPad Software Inc., San Diego, CA). The data are expressed as the mean ± S.D. Statistically significant differences among groups were analyzed using one-way analysis of variance (ANOVA) with Tukey's multiple comparison tests. P < 0:05 was considered statistically significant.

Results

HPLC profile of ZYP

The expression and distribution of F-actin in HUVECs were observed using a fluorescence microscope. The green and blue colors in Figure 3 correspond to F-actin and the nuclei, respectively. Based on the recorded images, the HUVECs in the X-ray group exhibit deformed F-actin, short pseudopodoid contraction, disordered microfilament arrangement, loose skeleton arrangement, poor directivity, coarse stress fiber formation in the cytoplasm with nucleus shrinkage, and rupture, unlike the cells in the control group. The observed features are characteristic of apoptotic cells. Pretreatment with ZYP (20–100 μg/mL) moderates the morphological changes listed above (Figure 3A). Compared to X-ray group cells, the cells in the ZYP group have fewer stress fibers, and more F-actin is distributed on the cell membranes. At higher concentrations of ZYP, the fluorescence intensity increases (Figure 3B), and the cell edges revert to smooth with irregular polygons, similar to the cells in the control group (Figure 3C).

Effect of ZYP on X-ray-induced changes in HUVEC membrane potential

Modified mitochondrial membrane potential is an early determinant of the mitochondrial apoptotic pathway. To determine the effect of ZYP on X-ray-induced HUVEC membrane potential, the fluorescence of rhodamine-labelled cells was analyzed. The images presented in Figures 4A and 4C demonstrate that compared to the control group, the cells in the X-ray treatment group exhibit significantly weakened intensity of green fluorescence ($P < 0.001$), which indicates that the mitochondrial membrane potential of these cells is reduced. ZYP treatment (20–100 μg/mL) partially alleviates the effect of X-ray exposure, as evidenced by the increased fluorescence intensity of ZYP-treated cells compared to X-ray group cells ($P < 0.001$). As shown in Figures 4B and 4D, changes in fluorescence intensity reflect changes in cell viability.

Overall, these findings indicate that ZYP prevents cell damage by affecting the mitochondrial membrane potential.

Effect of ZYP on X-ray-induced HUVEC apoptosis

The effect of ZYP on X-ray-induced HUVEC apoptosis was assessed by staining the cells in different groups with the Calcein-AM/PI double staining reagent then observing them using a fluorescence microscope. Upon entering the cytoplasm, Calcein-AM is hydrolyzed by esterase into green fluorescing Calcein. Meanwhile, the nuclear staining dye PI does not penetrate the cell membrane of living cells. Instead, it passes through the disordered regions of dead cell membranes, and upon reaching the nucleus, and embeds into the DNA double helix of the dead cells, thereby producing red fluorescence. The number of live and dead cells in different groups may thus be estimated based on the microscopic observation of green and red fluorescence signals, respectively. The images shown in Figure 5A demonstrate that compared to the control group, green fluorescence in the X-ray group is significantly reduced, whereas red fluorescence is enhanced. However, the green fluorescence intensity of cells in the ZYP group is higher than that detected for the X-ray group, and the red fluorescence intensity is lower.

To confirm that ZYP has a protective effect against X-ray-induced HUVEC apoptosis, Annexin V/PI flow cytometry experiments were conducted. As shown in Figure 5B, the percentage of apoptotic cells in the X-ray group (6 Gy) is 23.79%, which is much greater than that detected in the control group (2.34%). Pretreatment with 20 and 50 μg/mL ZYP effectively reduces the apoptosis rates to 14.92% and 9.32% ($P < 0.001$), respectively. The estimated total numbers of apoptotic cells in the early and late stages confirm that ZYP can protect HUVECs against X-Ray-induced apoptosis.

Effect of ZYP on ROS, malondialdehyde (MDA), lactate dehydrogenase (LDH), and superoxide dismutase (SOD) formation in HUVECs

The exposure of endothelial cells to X-ray radiation results in aseptic inflammation, which is normally caused by oxidative stress. Knowing that oxidative stress and the pro-inflammatory process are triggered by excessive ROS (metabolites of intracellular oxidation-reduction reactions) formation, the effect of ZYP on the number of reactive ROS in X-ray-induced HUVECs was evaluated, based on assessments of the MDA, SOD, and LDH levels. As shown in Figure 6A, the SOD level detected in the X-ray group is significantly less than that determined for the control group ($P < 0.001$). Contrarily, the LDH and MDA levels in cells exposed to X-ray radiation are significantly higher than those corresponding to control group cells ($P < 0.01$), as is the fluorescence intensity of ROS ($P < 0.001$) (Figures 6A, 6d, and 6E). Pretreatment with ZYP (20–100 μg/mL) reduces the fluorescence intensity of ROS ($P < 0.001$), the LDH level, and the MDA level (Figures 6B, 6D, and 6E), while increasing the content of SOD compared to the X-ray group. This effect is concentration-dependent (Figure 6C), and it indicates that ZYP has protective activity against the development of oxidative stress.

Effect of ZYP on the expression of apoptosis-related proteins in X-ray-induced HUVECs

The effect of ZYP pretreatment on the expression levels of the Bcl-2, Bax, caspase-9, and caspase-3 apoptosis-related proteins in X-ray-induced HUVECs was assessed. The obtained results indicate that X-ray exposure significantly increases the expression of Bax, caspase-9, and caspase-3 proteins compared to the control group (Figures 7C, 7d, and 7e), while decreasing the level of Bcl-2 (Figure 7B). However, pretreatment with ZYP reverses these effects by inhibiting the X-ray-induced expression of Bax, caspase-3, and caspase-9, and by increasing the level of Bcl2 (1.25 and 1.43-fold at 50 and 100 μg/mL ZYP, respectively). These results confirm that ZYP's effect on X-Ray-induced HUVEC apoptosis is related to the mitochondrial pathway.

Effect of ZYP on Nrf2, HO-1, and NQO1 levels

To further clarify the mechanism by which ZYP protects HUVECs against X-ray-induced injury, the expression levels of Nrf2, HO-1, and NQO1 in different groups were detected using western blot analyses. As shown in Figure 8, these levels are lower in the X-ray group than in the control group, but they significantly increase upon pretreatment with ZYP ($P < 0.05$). This indicates that ZYP can protect HUVECs against X-ray-induced oxidative injury through Nrf2/HO-1/NQO1 signaling.

Discussion

Cancer is one of the leading causes of morbidity and mortality worldwide, and has become a major global health concern. The World Health Organization (WHO) predicts that by 2030 an estimated 21.4 million new cases of cancer and 13.2 million cancer deaths will occur annually around the world [12]. Surgery, chemotherapy, and radiotherapy are the major conventional cancer treatments currently available [8]. Despite the effectiveness of chemoradiotherapy in some cases, its application is limited by high toxicity, normal tissue damage, and other side effects [4]. According to previous studies, therapies based on traditional Chinese medicine (TCM) improve the body's immune system function and are characterized by reduced side effects and increased sensitivity compared to chemoradiotherapy [8].

ZYP is an herbal mixture that is formulated based on the principles of Shenmai Powder and Danggui Buxue Decoction for the treatment of qi and blood deficiency [10, 13]. This TCM has been used clinically for more than 20 years, and it can effectively treat the qi and blood deficiency syndrome caused by radiotherapy and chemotherapy of malignant tumors [8]. Specifically, ZYP strengthens the body’s ability to resist damage, promotes blood generation, and inhibits bleeding. In this study, the fingerprint of the ZYP extract was established using high performance liquid chromatography (HPLC). The results show that the extract consists of five major components (ferulic acid, ginsenoside Rb1, ginsenoside Rg1, polyglucoside VII, and ginkgolide) whose anti-radiation effects have been previously reported. Radix Panacis Quinquefolii improves lung-yin, clears away deficiency fire, promotes fluid production, and quenches thirst [21]. Moreover, it restores the antioxidant enzymatic activity, cytokine level, and hormone level affected by IR in mice [22]. Meanwhile, Radix Angelicae Sinensis promotes blood circulation, relieves pain, replenishes the blood, and regulates menstruation [21]. It also enhances caspase-dependent apoptosis by down-regulating survivin, and increases the radiosensitivity of H22 cells to $^{12}C^{6+}$ heavy IR

[23]. Ferulic acid, the main active ingredient in ZYP, has anti-tumor and anti-inflammatory effects, and it protects against IR-induced apoptosis and oxidation via the ERK pathway [24]. As for Agrimony, it exhibits hemostasis, blood generation, malaria interception, detoxification, anti-oxidation, and anti-tumor activities [21]. In addition, agrimony lactone, the active ingredient in Agrimony, inhibits the proliferation of the human gastric adenocarcinoma AGS cell line [25]. Paris Polyphylla Smith presents detoxification, pain relief, and immunity regulation effects [21], whereas Polyphyllin I suppresses human osteosarcoma growth by inactivating the Wnt/β-actenin pathway in vitro and in vivo [26]. Radix Adenophorae nourishes the yin, moistens dryness, clears lung heat, cools the liver, and nurtures the bloo [21]. Based on the theory of TCM and existing research studies, ZYF can protect against radiation-induced injury of HUVECs.

Exposure to IR may lead to excessive production of reactive oxygen species, such as O_2^- (superoxide radical), OH (hydroxyl radical), and H_2O_2 (hydrogen peroxide), which in turn leads to increased intracellular oxidative stress [8]. The destruction of macromolecules, such as nucleic acids, proteins, and enzymes, under the effect of oxidative stress results in DNA chain rupture and reduced content and activity of anti-injury repair enzymes, as well as in changes in tissue morphology, metabolic function, and microcirculation [24, 27]. In this study, we show that the X-ray exposure promotes the excessive generation of ROS in HUVECs, which impairs the antioxidant mechanisms in these cells. To alleviate the effect of X-ray radiation, excess ROS must be eliminated [8]. In the cellular environment, free radicals are mainly removed by antioxidant enzymes such as SOD. The SOD metalloenzyme is prevalent in many organisms, and it is characterized by oxygen free radical scavenging activity. MDA is a degradation product of lipid peroxidation, and its content is directly related to the degree of lipid peroxidation in cells, which indirectly reflects the extent of cell damage [28, 29]. In the cellular environment, free radicals are mainly removed by antioxidant enzymes such as SOD. The SOD metalloenzyme is prevalent in many organisms, and it is characterized by oxygen free radical scavenging activity. MDA is a degradation product of lipid peroxidation, and its content is directly related to the degree of lipid peroxidation in cells, which indirectly reflects the extent of cell damage

The mitochondrion is an essential organelle that maintains the normal functioning of cells and that is in turn maintained by $\triangle\Psi m$ [30, 31]. Oxidative stress induces mitochondrial dysfunction, resulting in the transport of cytochrome C from the mitochondrial membrane to the cytoplasm. This triggers the activation of caspase-3 and caspase-9 enzymes in HUVECs, both of which are key cell death substrates that promote apoptosis [32]. The results obtained herein demonstrate that ZYP can partially protect against X-ray-induced (6 Gy) mitochondrial damage by inhibiting the expression of intracellular caspase-3 and caspase-9 proteins. This effect is dependent on the concentration of ZYP. Knowing that the contents of Bcl-2 and Bax (pro-apoptotic protein) in the outer membrane of the mitochondrion affect mitochondrial permeability, and that increased permeability promotes the transfer of apoptotic signals, the levels of Bcl-2 and Bax proteins in HUVECs were also assessed [24]. The results indicate that ZYP pretreatment alleviates the damaging effect of X-ray exposure on the mitochondrial membrane by regulating the expressions of Bax and Bcl-2, in addition to caspase-3 and caspase-9.

The key mechanism implicated in cellular antioxidant activity is the Nrf2/HO-1/NQO1 signaling pathway [33]. Nrf2 is a redox-sensitive transcription factor that is directly activated by ROS [19, 34]. Under normal circumstances, Nrf2 binds to Keap1(Kelch-like ECH-associated protein 1) and undergoes ubiquitination-dependent proteasome degradation. However, excessive ROS production (oxidative stress) induces a conformational change in Keap1 (modification of some sensor cysteines), which interferes with its binding to Nrf2. The disruption of Nrf2/Keap1 binding promotes the transfer of the accumulated Nrf2 protein to the nucleus, where it activates the HO-1, NQO1, and SOD target genes [35]. Under normal circumstances, Nrf2 binds to Keap1(Kelch-like ECH-associated protein 1) and undergoes ubiquitination-dependent proteasome degradation. However, excessive ROS production (oxidative stress) induces a conformational change in Keap1 (modification of some sensor cysteines), which interferes with its binding to Nrf2. The disruption of Nrf2/Keap1 binding promotes the transfer of the accumulated Nrf2 protein to the nucleus, where it activates the HO-1, NQO1, and SOD target genes [33]. Overall, Nrf2 is responsible for maintaining redox homeostasis and regulating cell antioxidant reduction. Previously, it had been shown that curcumin protects against liver injury in irradiated rats by modulating the therapeutic targets of Nrf2 [36]. NQO1, an important downstream phase II detoxification enzyme regulated by Nrf2, can also reduce oxidative damage by catalyzing the double-electron reduction of quinones, nitroxides, and other compounds [37]. Salidroside increases the protein expressions of HO-1 and NQO1, resulting in significantly reduced H_2O_2-induced oxidative stress injury of HUVECs [35]. Similarly, our results show that the protein expressions of Nrf2, HO-1, and NQO1 in irradiated cells pretreated with ZYP are significantly increased. This indicates that ZYP promotes cell survival, restricts apoptosis, and inhibits X-ray-induced oxidative stress by regulating the Nrf2/HO-1/NQO1 signaling pathway.

Conclusion

This study establishes that ZYP can protect against X-ray-induced injury of HUVECs by mediating ROS scavenging, activating the Nrf2/HO-1/NQO1 signaling pathway, and stabilizing the mitochondrial membrane. This suggests that the X-ray-protection activity of ZYP is attributed to its antioxidative ability. To confirm the protective effect of ZYP on bodies exposed to X-ray radiation, further studies must be conducted, particularly in vivo studies.

Abbreviations

ZYP: Zhengyuan prescription

HUVECs: Human umbilical vein endothelial cell

ROS: Reactive oxygen species

Bcl-2: B-cell lymphoma 2

Bax : Bcl-2-associated X protein

Nrf2: Nuelear Faetor-E2-related faetor 2

HO1: Heme oxygenase 1

NQO1: NAD(P)H dehydrogenase quinone 1

TCM: Traditional Chinese medicine

MTT:3-(4,5-dimethyl-2-thiazolyl)-2,5-diphenyl-2-H-tetrazolium bromide

DMSO: Dimethyl sulfoxide

FITC: Fluorescein isothiocyanate isomer

MDA: Malondialdehyde

SOD: Superoxide dismutase

LDH: Lactate dehydrogenase

HPLC: High performance liquid chromatography

DMEM: Dulbecco's modified Eagle's medium

FBS: Fetal bovine serum

BCA: Bicinchoninic acid

RIPA: Radioimmunoprecipitationassay

PVDF: Polyvinylidene fluoride

ECL: Enhanced chemiluminescence

Keap 1: Kelch-like ECH-associated protein 1

Declarations

Availability of data and materials

The research data generated from this study is included within the article.

Acknowledgments

We thank LetPub (www.letpub.com) for its linguistic assistance during the preparation of this manuscript.

Funding

This research was funded by the Major Project of National Science and Technology on New Drug Creation (2019ZX09301133), National Natural Science Foundation (81703777) and Special Fund Project for Construction of Modern Agricultural Industry Technology System (CARS-21).

Contributions

Yalei Pan and Zhishu Tang designed the research; Xiaoni Cheng, Haichao Zhang and Jie Su conducted experiments; Rui Zhou and Jian Ni analyzed data and interpreted results of experiments; Yalei Pan and Xiaoni Cheng drafted manuscript. All authors revised the final manuscript and all authors read and approved the final manuscript.

Corresponding author

Corresponding author Correspondence to Yalei Pan and Zhishu Tang

Ethics declarations

Availability of data and materials

The data used to support the findings of this study are available from the corresponding author upon request.

Competing interests

The authors declare that they have no conflicts of interest.

Consent for publication

No application

References

1. Favareto SL, Pellizzon ACA, Lopes Pinto CA, Bertolli E, Castro DG. The Role of Radiation Therapy as an Adjuvant Treatment in Nodal Metastasis of Malignant Chondroid Syringoma. *Cureus* 2020, 12(11):e11360.
2. Smith T, O'Cathail SM, Silverman S, Robinson M, Tsang Y, Harrison M, Hawkins MA. Stereotactic Body Radiation Therapy Reirradiation for Locally Recurrent Rectal Cancer: Outcomes and Toxicity. *Adv Radiat Oncol* 2020, 5(6):1311-1319.
3. Javvadi P, Segan AT, Tuttle SW, Koumenis C. The chemopreventive agent curcumin is a potent radiosensitizer of human cervical tumor cells via increased reactive oxygen species production and overactivation of the mitogen-activated protein kinase pathway. *Mol Pharmacol* 2008, 73(5):1491-1501.

4. Citrin D, Cotrim AP, Hyodo F, Baum BJ, Krishna MC, Mitchell JB. Radioprotectors and mitigators of radiation-induced normal tissue injury. *Oncologist* 2010, 15(4):360-371.
5. Liu WY, Zhang JW, Yao XQ, Jiang C, He JC, Ni P, Liu JL, Chen QY, Li QR, Zang XJ *et al*. Shenmai injection enhances the cytotoxicity of chemotherapeutic drugs against colorectal cancers via improving their subcellular distribution. *Acta Pharmacol Sin* 2017, 38(2):264-276.
6. Wang Q, Xie C, Xi S, Qian F, Peng X, Huang J, Tang F. Radioprotective Effect of Flavonoids on Ionizing Radiation-Induced Brain Damage. *Molecules* 2020, 25(23):5719.
7. Robbins ME, Brunso-Bechtold JK, Peiffer AM, Tsien CI, Bailey JE, Marks LB. Imaging radiation-induced normal tissue injury. *Radiat Res* 2012, 177(4):449-466.
8. Zhang QY, Wang FX, Jia KK, Kong LD. Natural Product Interventions for Chemotherapy and Radiotherapy-Induced Side Effects. *Frontiers in Pharmacology* 2018, 9.
9. Li S, So TH, Tang G, Tan HY, Wang N, Ng BFL, Chan CKW, Yu EC, Feng Y. Chinese Herbal Medicine for Reducing Chemotherapy-Associated Side-Effects in Breast Cancer Patients: A Systematic Review and Meta-Analysis. *Front Oncol* 2020, 10:599073.
10. Lo LC, Chen CY, Chen ST, Chen HC, Lee TC, Chang CS. Therapeutic efficacy of traditional Chinese medicine, Shen-Mai San, in cancer patients undergoing chemotherapy or radiotherapy: study protocol for a randomized, double-blind, placebo-controlled trial. *Trials* 2012, 13:232.
11. Qi F, Zhao L, Zhou A, Zhang B, Li A, Wang Z, Han J. The advantages of using traditional Chinese medicine as an adjunctive therapy in the whole course of cancer treatment instead of only terminal stage of cancer. *Biosci Trends* 2015, 9(1):16-34.
12. Qi F, Li A, Inagaki Y, Gao J, Li J, Kokudo N, Li X-K, Tang W. Chinese herbal medicines as adjuvant treatment during chemo- or radio-therapy for cancer. *Biosci Trends* 2010, 4(6):297-307.
13. Gao QT, Cheung JK, Choi RC, Cheung AW, Li J, Jiang ZY, Duan R, Zhao KJ, Ding AW, Dong TT *et al*. A Chinese herbal decoction prepared from Radix Astragali and Radix Angelicae Sinensis induces the expression of erythropoietin in cultured Hep3B cells. *Planta Med* 2008, 74(4):392-395.
14. Qu YH, Wang PY, Wang XJ, Tang ZS, Tang JQ. Protective effect of Zhengyuan Prescription on mice injured by 60Co-γ ray irradiation. *Chinese Traditional Patent Medicine* 2014, 36, 468-473.
15. Helm A, Lee R, Durante M, Ritter S. The Influence of C-Ions and X-rays on Human Umbilical Vein Endothelial Cells. *Frontiers in Oncology* 2016, 6.
16. Sharma P, Templin T, Grabham P. Short term effects of gamma radiation on endothelial barrier function: uncoupling of PECAM-1. *Microvasc Res* 2013, 86:11-20.
17. Schröder S, Juerß D, Kriesen S, Manda K, Hildebrandt G. Immunomodulatory properties of low-dose ionizing radiation on human endothelial cells. *Int J Radiat Biol* 2019, 95(1):23-32.
18. Gabryś D, Greco O, Patel G, Prise KM, Tozer GM, Kanthou C. Radiation effects on the cytoskeleton of endothelial cells and endothelial monolayer permeability. *Int J Radiat Oncol Biol Phys* 2007, 69(5):1553-1562.

19. Baselet B, Sonveaux P, Baatout S, Aerts A. Pathological effects of ionizing radiation: endothelial activation and dysfunction. *Cellular and Molecular Life Sciences* 2018, 76(4):699-728.
20. Huang Q, Zhou Z, Yan F, Dong Q, Wang L, Sha W, Xu Q, Zhu X, Zhao L. Low-dose X-ray irradiation induces morphological changes and cytoskeleton reorganization in osteoblasts. *Exp Ther Med* 2020, 20(6):283.
21. The State Pharmacopoeia Commission of the People's Republic of China. Pharmacopoeia of the People's Republic of China 2015. *China Chemical Industry Press B,* China, 2015.
22. Liao D, Jia C, Sun P, Qi J, Li X. Quality evaluation of Panax quinquefolium from different cultivation regions based on their ginsenoside content and radioprotective effects on irradiated mice. *Sci Rep* 2019, 9(1):1079.
23. Kou W, Li YD, Liu K, Sun SB, Dong YM, Wu ZH. Radix Angelicae Sinensis and Radix Hedysari enhance radiosensitivity of $^{12}C^{6+}$ radiation in human liver cancer cells by modulating apoptosis protein. *Saudi Med J* 2014, 35(9):945-952.
24. Ma ZC, Hong Q, Wang YG, Tan HL, Xiao CR, Liang QD, Wang DG, Gao Y. Ferulic acid protects lymphocytes from radiation-predisposed oxidative stress through extracellular regulated kinase. *Int J Radiat Biol* 2011, 87(2):130-140.
25. Teng H, Huang Q, Chen L. Inhibition of cell proliferation and triggering of apoptosis by agrimonolide through MAP kinase (ERK and p38) pathways in human gastric cancer AGS cells. *Food Funct* 2016, 7(11):4605-4613.
26. Chang J, Li Y, Wang X, Hu S, Wang H, Shi Q, Wang Y, Yang Y. Polyphyllin I suppresses human osteosarcoma growth by inactivation of Wnt/β-catenin pathway in vitro and in vivo. *Scientific Reports* 2017, 7(1).
27. Ji HJ, Wang DM, Wu YP, Niu YY, Jia LL, Liu BW, Feng QJ, Feng ML. Wuzi Yanzong pill, a Chinese polyherbal formula, alleviates testicular damage in mice induced by ionizing radiation. *BMC Complementary and Alternative Medicine* 2016, 16(1).
28. Xie Y, Guo Y, Cao S, Xue M, Fan Z, Gao C, Jin B. Hydroxysafflor Yellow A Attenuates Hydrogen Peroxide-Induced Oxidative Damage on Human Umbilical Vein Endothelial Cells. *Evid Based Complement Alternat Med* 2020, 2020:8214128.
29. Du J, Yin G, Hu Y, Shi S, Jiang J, Song X, Zhang Z, Wei Z, Tang C, Lyu H. Coicis semen protects against focal cerebral ischemia-reperfusion injury by inhibiting oxidative stress and promoting angiogenesis via the TGFβ/ALK1/Smad1/5 signaling pathway. *Aging (Albany NY)* 2020, 12.
30. Sun Z, Lan X, Ahsan A, Xi Y, Liu S, Zhang Z, Chu P, Song Y, Piao F, Peng J *et al*. Phosphocreatine protects against LPS-induced human umbilical vein endothelial cell apoptosis by regulating mitochondrial oxidative phosphorylation. *Apoptosis* 2016, 21(3):283-297.
31. La Sala L, Mrakic-Sposta S, Micheloni S, Prattichizzo F, Ceriello A. Glucose-sensing microRNA-21 disrupts ROS homeostasis and impairs antioxidant responses in cellular glucose variability. *Cardiovascular Diabetology* 2018, 17(1).

32. Wang Y, Kong L, Wu T, Tang M. Urban particulate matter disturbs the equilibrium of mitochondrial dynamics and biogenesis in human vascular endothelial cells. *Environ Pollut* 2020, 264:114639.
33. Zhu Y, Zhang YJ, Liu WW, Shi AW, Gu N. Salidroside Suppresses HUVECs Cell Injury Induced by Oxidative Stress through Activating the Nrf2 Signaling Pathway. *Molecules* 2016, 21(8).
34. Zhou R, Long H, Zhang B, Lao Z, Zheng Q, Wang T, Zhang Y, Wu Q, Lai X, Li G *et al*: Salvianolic acid B, an antioxidant derived from Salvia militarize, protects mice against gammaradiationinduced damage through Nrf2/Bach1. *Mol Med Rep* 2019, 19(2):1309-1317.
35. Shen T, Li HZ, Li AL, Li YR, Wang XN, Ren DM. Homoeriodictyol protects human endothelial cells against oxidative insults through activation of Nrf2 and inhibition of mitochondrial dysfunction. *Vascul Pharmacol* 2018, 109:72-82.
36. Eassawy MMT, Salem AA, Ismail AFM. Biochemical study on the protective effect of curcumin on acetaminophen and gamma-irradiation induced hepatic toxicity in rats. *Environ Toxicol* 2020.
37. Shi J, Zhang M, Zhang L, Deng H. Epigallocatechin-3-gallate attenuates microcystin-LR-induced apoptosis in human umbilical vein endothelial cells through activation of the Nrf2/HO-1 pathway. *Environ Pollut* 2018, 239:466-472.

Tables

Table 1 Composition of ZYP.

Components	Ratio
Radix Angelicae Sinensis	8
Radix Panacis Quinquefolii	25
Herba Agrimoniae	25
Paris polyphylla	10
Adenophora tetraphylla	12.5

Table 2 Antibodies used for western blotting.

Primary antibody name	Dilution	Manufacturer	Catalog number
Bax	1:1,000	CST	5023
Bcl-2	1:1,000	CST	15071
Caspase-3	1:1,000	CST	14220
Caspase-9	1:1,000	CST	9508
Nrf2	1:1,000	Proteintech	16396
HO-1	1:1,000	Proteintech	27282
NQO1	1:1,000	Proteintech	11451
β-actin	1:1,000	CST	3700

Figures

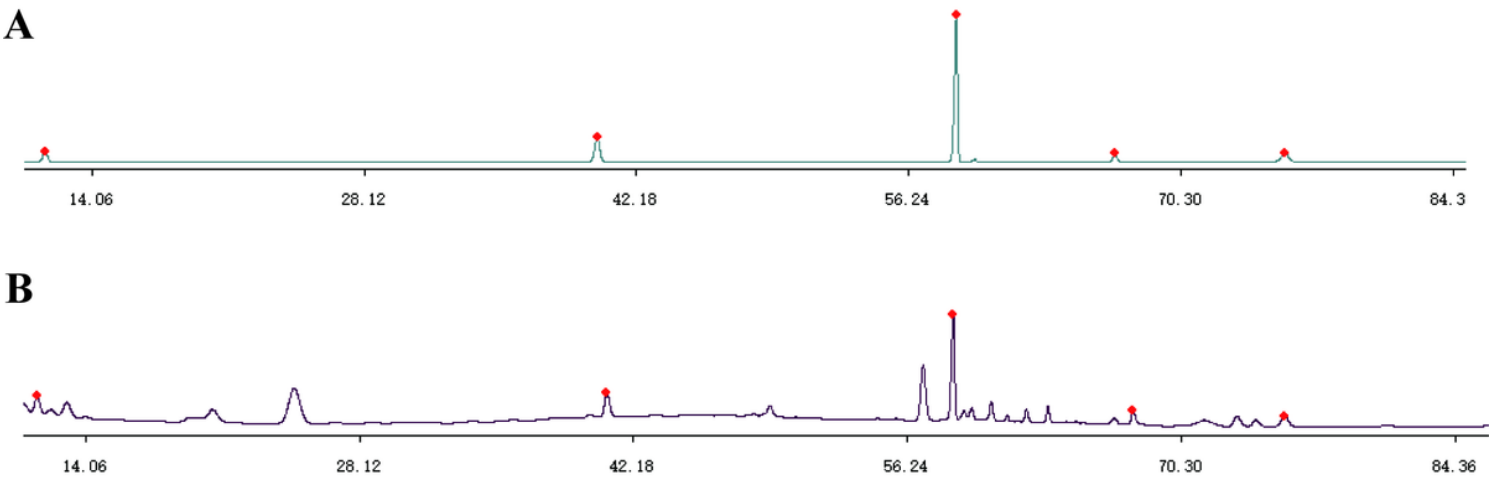

Figure 1

The HPLC chromatograms of ZYP. (A) HPLC chromatogram of mixed reference substances. (B) HPLC reference fingerprint of ZYP. (Ferulic acid (1), ginsenoside Rg1 (2), ginsenoside Rb1(3), polyphyllin VI (4) and agrimonolide (5)).

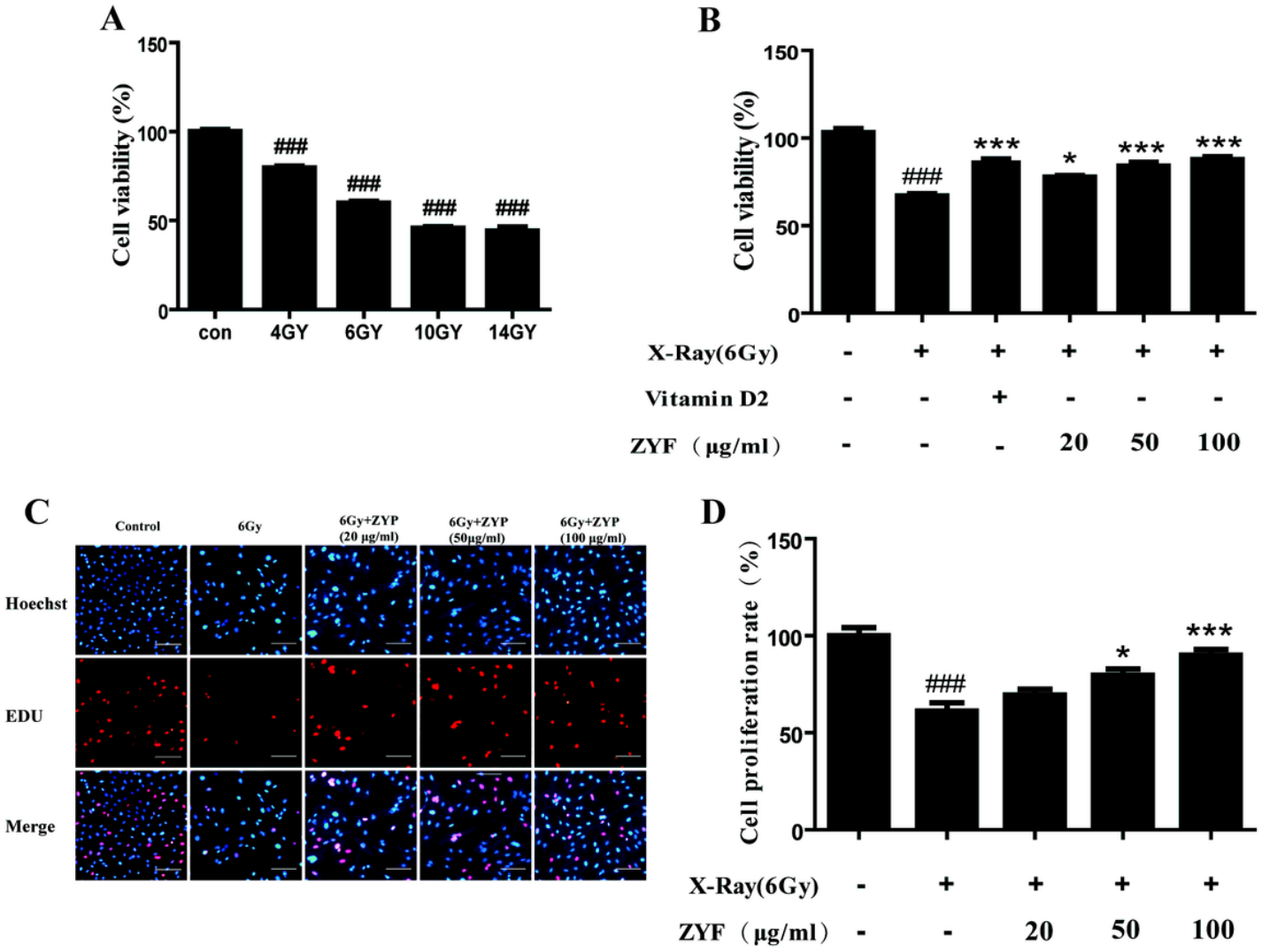

Figure 2

(A) Effect of ZYP on the survival rate of X-ray-induced HUVECs (cells exposed with 0–14 Gy X-ray radiation for 48 h). #P < 0.05, ##P < 0.01, and ###P < 0.001 vs. control. (B) Protective effect of ZYP pretreatment on X-ray-induced HUVEC damage (cells treated with 20–100 μg/mL ZYP then exposed to 6 Gy X-ray radiation). (C) Fluorescence images of EDU-stained cells showing the proliferation and apoptosis of HUVECs (x100 magnification). (D) Cell proliferation rate. ###P <0.001 vs. control group only; *P < 0.05 and ***P < 0.001 vs. X-ray group only.

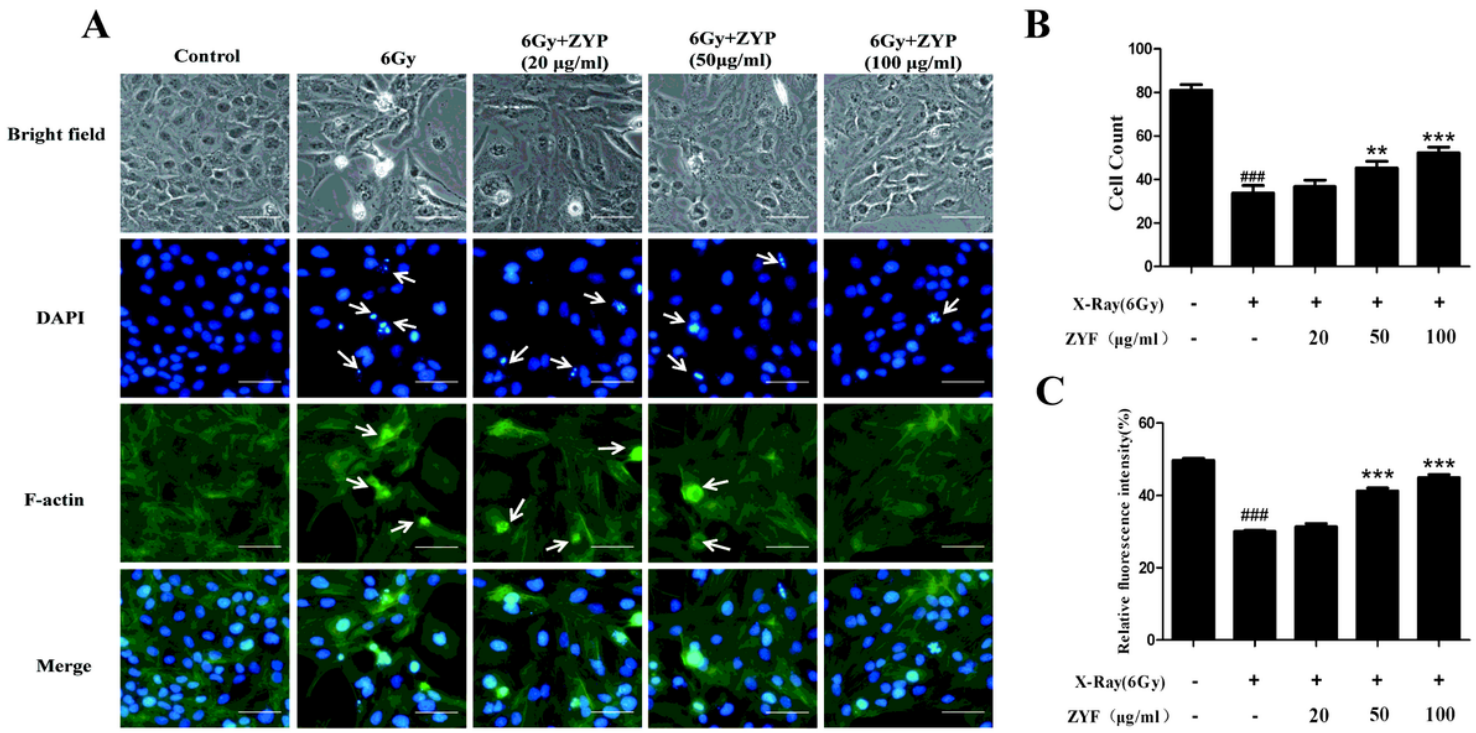

Figure 3

(A) Fluorescence images showing the effect of ZYP on X-ray-induced morphological changes in HUVECs (x200 magnification). The arrows point to HUVECs with apoptotic nuclei. (B) Cell count. (C) Relative fluorescence intensity (relative to the control group). ###P < 0.001 vs. control group only; **P < 0.01 and ***P < 0.001 vs. X-ray group only.

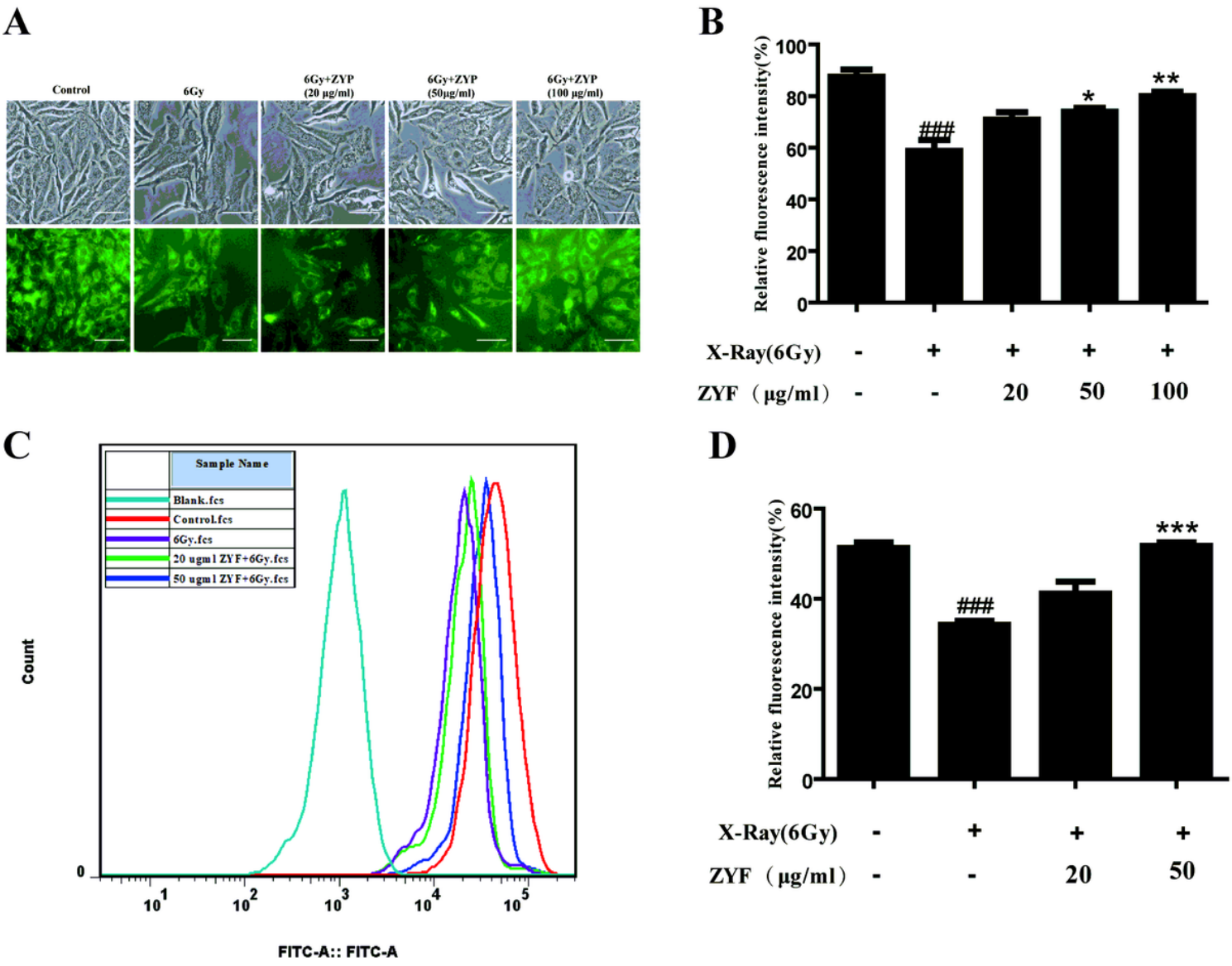

Figure 4

Effect of ZYP on X-ray-induced changes in HUVEC mitochondrial membrane potential. (A) Fluorescence images of cells stained with rhodamine 123 (x200 magnification). (B) Relative fluorescence intensity (relative to the control group). (C) Flow cytometry assessment of the mitochondrial membrane potential of cells. (D) Quantitative analysis of the fluorescence intensity in (C). ###P < 0.001 vs. control group only; *P < 0.05 and **P < 0.01 vs. X-ray group only.

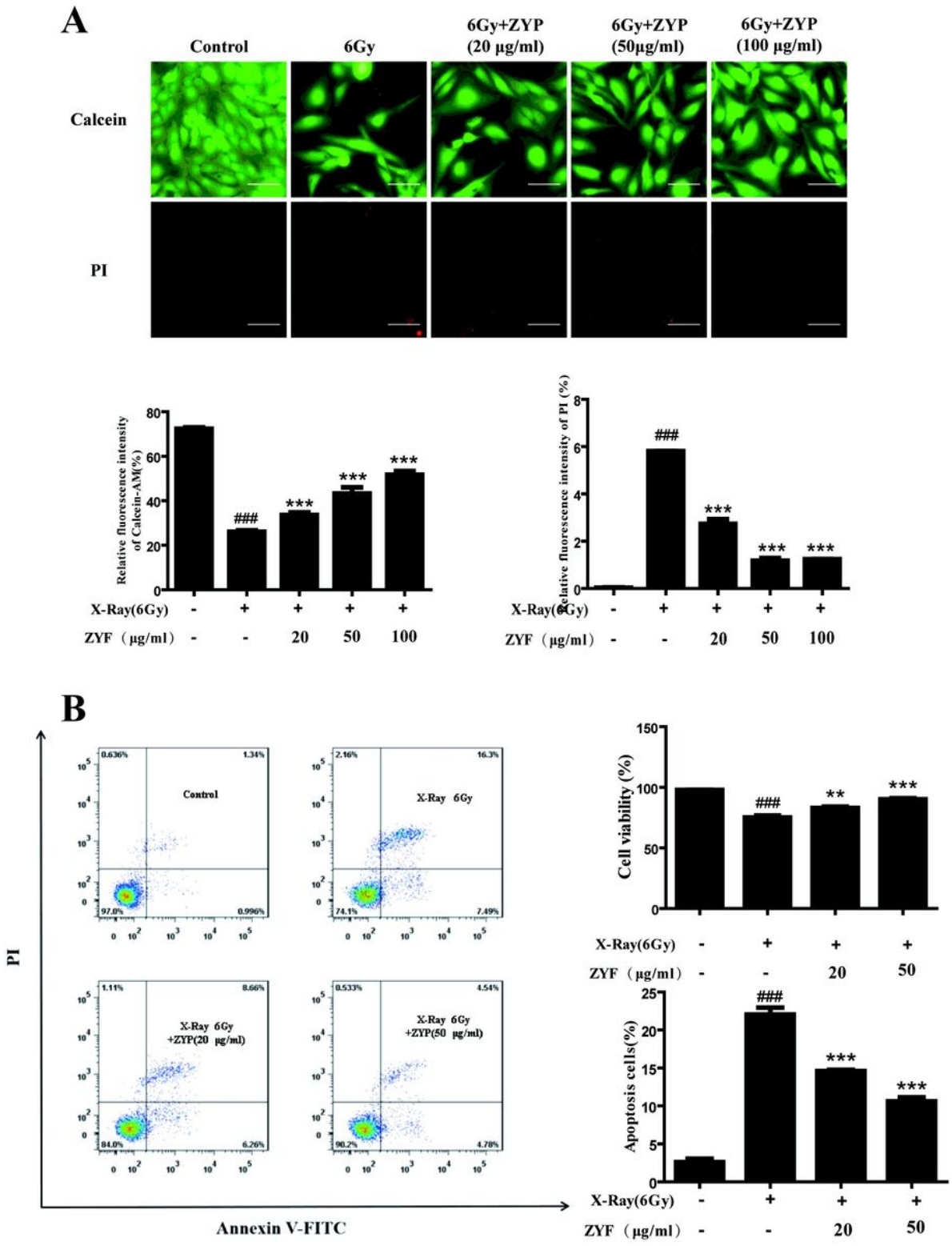

Figure 5

Effect of ZYP on the X-ray-induced apoptosis of HUVECs. (A) Calcein/PI cell assay (calcein stains living cells and PI stains dead cells). (B) Flow cytometry analysis. The lower right corner indicates the proportion (%) of early apoptotic cells, while the upper right corner indicates the proportion (%) of late apoptotic cells. ###P < 0.001 vs. the control group only; **P < 0.01 and ***P < 0.001 vs. the X-ray group only.

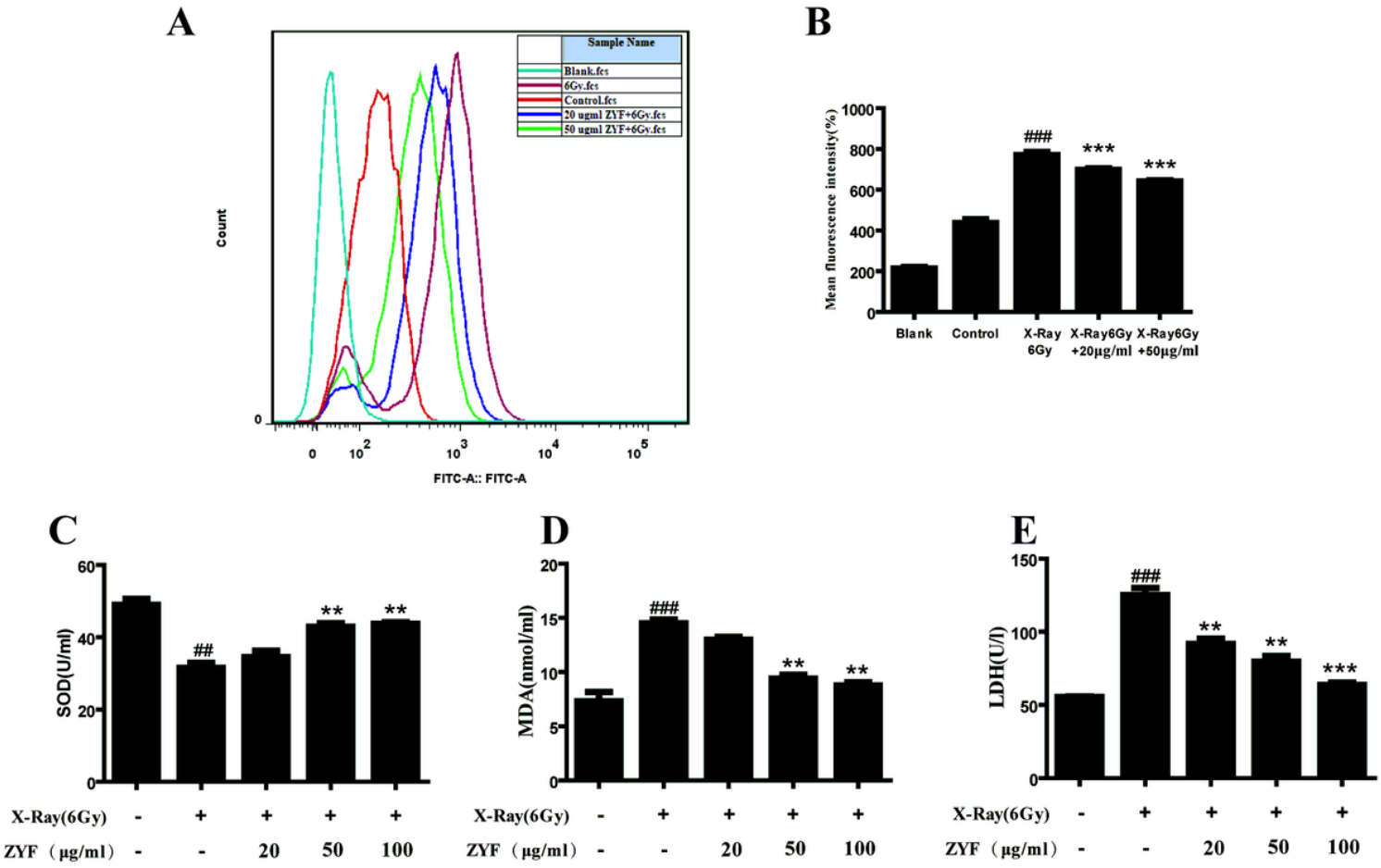

Figure 6

Effect of ZYP on the formation of ROS, MDA, LDH, and SOD in HUVECs. (A) Representative flow cytometry images of intracellular ROS levels. (B) Quantitative analysis of the fluorescence intensity in (a). Quantitative analysis of intracellular (C) LDH, (D) MDA, and (E) SOD levels. Data are expressed as mean ± SD. ##P < 0.01 and ###P < 0.001 vs. the control group only; *P < 0.05, **P < 0.01 and ***P < 0.001 vs. the X-ray group only.

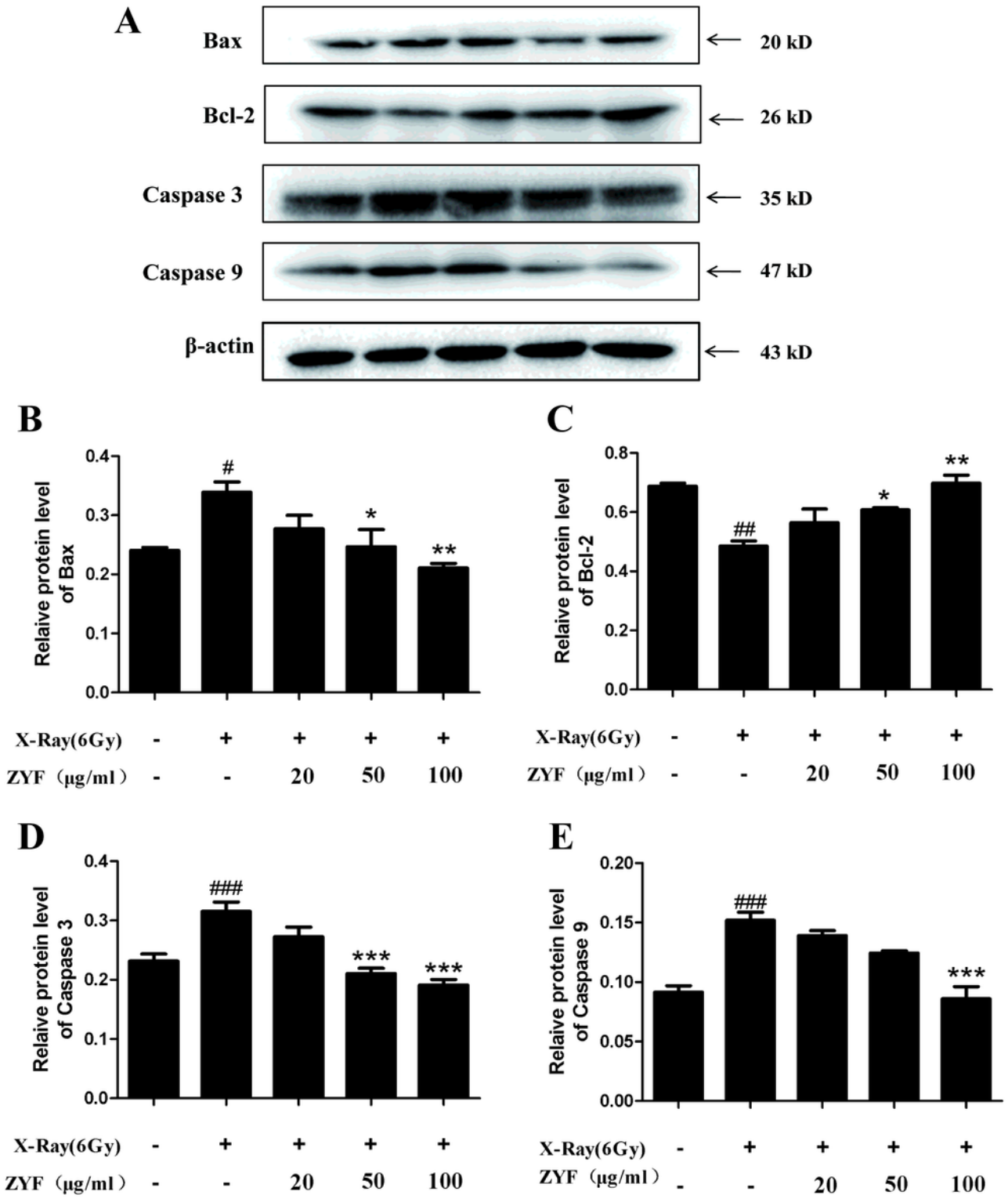

Figure 7

Effect of ZYP on the expression of apoptosis-related proteins in X-ray-induced HUVECs. Cells were pretreated with 20–100 μg/mL ZYP for 3 h, followed by treatment with 6 Gy X-ray for 48 h. (A) Western blot analysis of Bax, Bcl-2, caspase-3, and caspase-9 protein expressions. Quantification of (B) Bax, (C) Bcl-2, (D) caspase-3, and (E) caspase-9 levels (grey scale analysis). #P < 0.05, ##P < 0.05, and ###P < 0.001 vs. the control group only; *P < 0.05, **P < 0.01, and ***P < 0.001 vs. the X-ray group only.

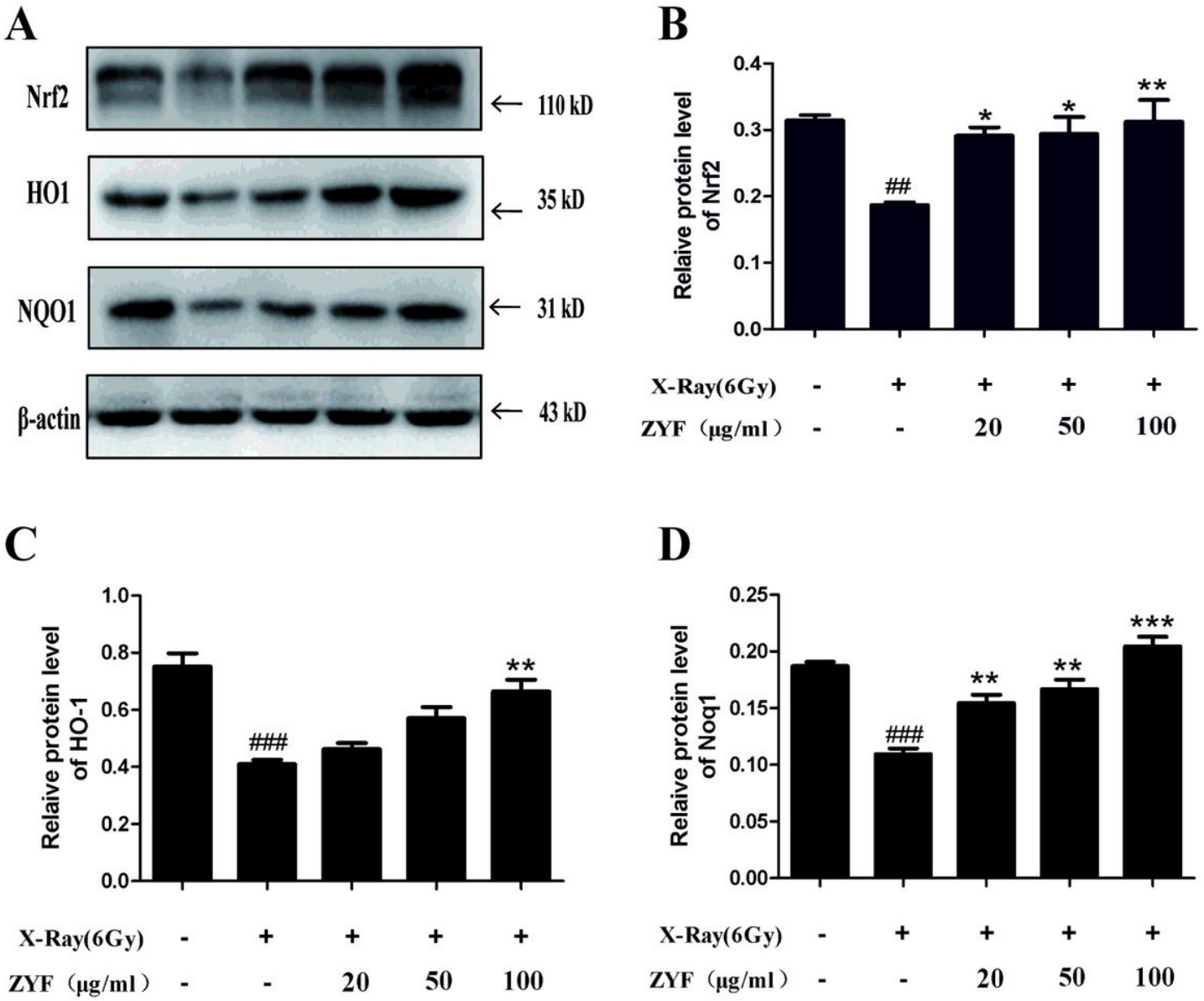

Figure 8

Effect of ZYP on Nrf2/HO-1/NQO1 signaling in X-ray-induced HUVECs. Cells were pretreated with 20–100 μg/mL ZYP for 3 h, followed by treatment with 6 Gy X-Ray for 48 h. (A) Western blot analysis of Nrf2, HO-1, and NQO1 protein expressions. (B) Quantification o protein levels (grey scale analysis). ##P < 0.05 and ###P < 0.001 vs. the control group only; *P < 0.05, **P < 0.01, and ***P < 0.001 vs. the X-ray group only.